Letter

Doping the Mott insulating state of the triangular-lattice Hubbard model reveals the Sordi transition

P.-O. Downey,[1] O. Gingras,[2] C.-D. Hébert,[1] M. Charlebois,[3] and A.-M. S. Tremblay[1,*]
[1]*Département de Physique and Institut Quantique, Université de Sherbrooke, Québec, Canada J1K 2R1*
[2]*Center for Computational Quantum Physics, Flatiron Institute, 162 Fifth Avenue, New York, New York 10010, USA*
[3]*Département de Biochimie, Chimie, Physique et Science Forensique, Institut de Recherche sur l'Hydrogène, Université du Québec à Trois-Rivières, Trois-Rivières, Québec, Canada G9A 5H7*

(Received 20 July 2023; revised 20 June 2024; accepted 29 August 2024; published 12 September 2024)

It has been reported that upon doping a Mott insulator, there can be a crossover to a pseudogapped metallic phase followed by a first-order transition to another thermodynamically stable metallic phase. We call this first-order metal-metal transition the Sordi transition. It was argued that the initial reports of Sordi transitions at finite temperature could be explained by finite size effects and biases related to the model and method used. In this work, we report the Sordi transition on larger clusters at finite temperature on a triangular lattice, where long-range antiferromagnetic fluctuations are frustrated, using a different method, the dynamical cluster approximation instead of the cellular dynamical mean-field theory. This demonstrates that this first-order transition is a directly observable transition in doped Mott insulators and that it is relevant for experiments on candidate spin-liquid organic materials.

DOI: 10.1103/PhysRevB.110.L121109

Emergent states of strongly correlated electronic systems are among the most fascinating phenomena in physics. Simple models can capture the essence of intriguing correlated states while remaining interpretable. The Hubbard model [1–5], although extremely simple to write and credited with important successes, still has no exact solution in two dimensions (2D) and remains a source of important challenges.

Hubbard already understood that this model should contain the physics of the so-called Mott transition, namely a transition from a metal to an insulator caused by strong electronic repulsion. By now, numerous experiments have suggested that there is such an interaction-driven transition in the half-filled single-band model and that it is first order [6–13], a result supported by various embedding methods such as dynamical mean field theory (DMFT) [14–18] and its multisite extensions: cluster DMFT (CDMFT) [19–21] and the dynamical cluster approximation (DCA) [22–24].

Here we focus on the doping-driven Mott transition. Early on, several works have suggested that, upon changing the chemical potential μ away from half-filling, the electronic compressibility, $\partial n/\partial\mu$ with n the average number of electron per site, displays hysteresis characteristic of a first-order transition [25–29]. There is, however, disagreement on the nature of the phases that are linked by doping-driven transitions. Single-site DMFT [25] finds a first-order transition between the Mott insulator (MI) and the metal, while DCA cluster calculations find momentum space differentiation [30] or a first-order transition on the electron-doped side only when the model is frustrated [26,27,31]. In contrast, Ref. [28] found that a first-order doping-driven transition could connect two thermodynamically stable metallic phases at finite temperature [32]: a pseudogap (PG) phase and a correlated Fermi liquid (cFL). We refer to this type of doping-driven transition as the Sordi transition.

This transition could have profound implications as it appears to be the hallmark of the onset of a strongly correlated PG [33,34], namely a pseudogap that is a consequence only of short-range spin correlations [35,36], not of long-wavelength spin fluctuations [37]. What is meant by pseudogap in this work simply refers to the appearance of a local minimum in the density of states, exemplified in Fig. 1(b) and quantified in the Supplemental Material [38]. Notice that the PG phase is different from the bad-metal or bad-insulator phases discussed in single-site DMFT [18,39] since in these high-temperature phases one does not observe sharp peaks surrounding the minimum at the Fermi level. In short, it is a phase where density of states and spin susceptibility are reduced and where various features appear in transport. Its onset for decreasing temperature happens at $T^*(p)$ that depends on doping p. The Sordi transition also explains several features of the pseudogap in cuprates [34,40–46], for example the experimentally observed sudden drop of T^* at a critical doping p^* [47,48], critical opalescence [46,49], the specific heat maximum [44,50] plus logarithmic temperature dependence [42,50], and even possibly high temperature linear scattering rate [45,51].

More generally, the Sordi transition can be defined as a first-order transition between a strongly correlated metal and a weakly correlated metal. It is important to contrast the first-order nature of such a transition to general doping-driven transitions [17,25,26,29,30,52–56].

The Sordi transition was first reported in Ref. [28] using CDMFT on the 2D square lattice single-band Hubbard model with only nearest neighbor hopping t. In Ref. [57], the transition has also been seen when including a next-nearest hopping

*Contact author: andre-marie.tremblay@usherbrooke.ca

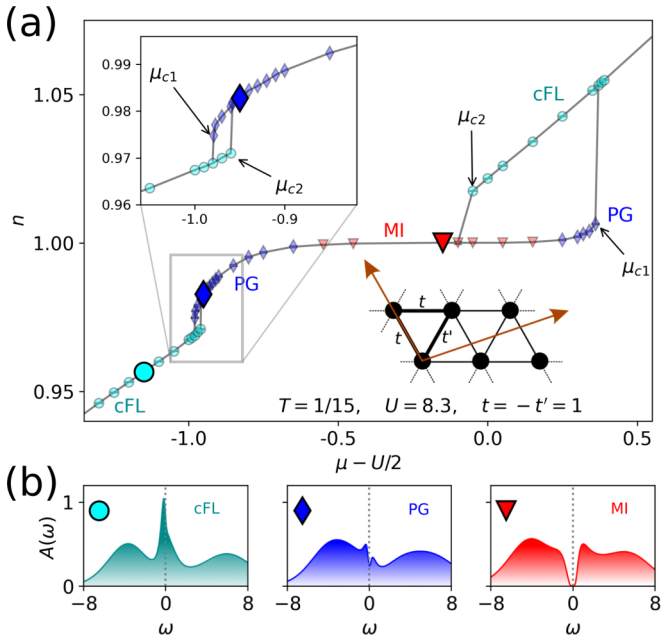

FIG. 1. (a) First-order doping-driven Sordi transitions at $U = 8.3$ and $T = 1/15$. The hole-doped Sordi transition is highlighted in the inset. We define the quantities μ_{c1} and μ_{c2} as the critical μ for the transition from the Mott insulator (MI) or pseudogap (PG) to correlated Fermi liquid (cFL), and from cFL to MI or PG, respectively. The Sordi transition corresponds to a first-order transition that evolves from the Mott transition at half-filling but that occurs between two stable metallic states. The cluster used on the real lattice is displayed in the lower right corner. (b) Local spectral weight for the representative points of (a). We use the spectral weight to classify the states obtained by the calculations. More details can be found in the Supplemental Material [38].

term $t' = -0.1t$. Similar phenomena have been observed in different contexts [53–55,58].

Objections that have been raised to the physical relevance of the Sordi transition include the fact that in real systems, this transition could be hidden by long-range ordered phases or by long-range correlations precursors of zero-temperature ordered phases. The latter argument has also been presented against the interaction-driven Mott transition [59]. It has also been argued that the Sordi transition could be an artifact of CDMFT on a small 2×2 square cluster, as it overemphasizes singlet correlations.

Here we study the Sordi transition on the triangular lattice. While several magnetic phases appear at zero temperature for values of interaction slightly larger than the Mott transition [60], the triangular lattice geometrically forbids long-range magnetic correlations until very low temperature, in particular for the range of interaction strengths of interest to us: $8.5 \leqslant U/t \leqslant 10.54$ [61–71]. We also find that the strong coupling metallic phase is a PG phase in the triangular lattice away from half-filling [38].

In this Letter, we achieve two broad goals.

(i) First, we show that the Sordi transition is not an artifact of either (a) the square lattice, since we work on the triangular lattice; (b) nor of CDMFT, since we use DCA; (c) nor of four-site clusters, since we study six-site clusters; (d) nor of long-correlation lengths, since magnetism is frustrated on the triangular lattice. We instead confirm that the transition is related to Mott physics, namely strong interactions, and that it should be observable at $T > 0$.

(ii) Second, we map out the phase diagram as a function of interaction U and chemical potential μ for two different temperatures and identify possibly observable pseudogap regions, in particular in spin-liquid candidate κ-BEDT layered organic compounds [72–74].

The model. We investigate the one-band 2D Hubbard model [75–78], defined by the Hamiltonian

$$H = -\sum_{i,j,\sigma} t_{ij} \hat{c}^{\dagger}_{i\sigma} \hat{c}_{j\sigma} + U \sum_{i} \hat{n}_{i\uparrow} \hat{n}_{i\downarrow} - \mu \sum_{i\sigma} \hat{n}_{i\sigma}, \qquad (1)$$

where t_{ij} represents the hopping terms between sites i and j, $\hat{c}^{\dagger}_{i\sigma}$ and $\hat{c}_{i\sigma}$ are respectively the creation and annihilation operators for electrons with spin σ at site i, U is the strength of the on-site Coulomb interaction between electrons, $\hat{n}_{i\sigma} = \hat{c}^{\dagger}_{i\sigma} \hat{c}_{i\sigma}$ is the number operator for electrons with spin σ at site i, and μ is the chemical potential. The six-site cluster that we study is shown in Fig. 1(a). We consider only the nearest-neighbor hopping terms t and t', where t' is useful to model the anisotropic triangular lattice and looks like a second-neighbor hopping when the lattice is mapped on a set of orthogonal basis vectors. Here we take $t = -t' = 1$. These signs of the hopping terms were chosen with the cuprate convention. At half-filling, the sign of t' is irrelevant and, in general, changing it is equivalent to a particle-hole transformation [79]. We work in units where hopping t, lattice spacing, and Planck and Boltzmann constants are unity.

The solutions to this model are obtained using a state-of-the-art DCA implementation [80–82] with continuous-time auxiliary-field quantum Monte Carlo interaction expansion (CT-AUX) [83,84]. The six-site cluster on Fig. 1 was shown in Refs. [23,45] to exhibit the major features seen in its larger counterpart (12 sites). Note that, contrarily to CDMFT, the DCA cluster has periodic boundary conditions on the cluster.

Filling induced first-order transitions. Figure 1 presents the first-order doping-driven transitions obtained on both the hole- and electron-doped sides, for $U = 8.3$ and $T = 1/15$. The hole-doped doping-driven transition highlighted in the inset is clearly a Sordi transition since it shows a first-order transition between two metallic (compressible) states away from half-filling. As in the careful studies of Refs. [28] and [29] on the square lattice, observing this transition requires very fine scans in μ and might have been missed in earlier studies [26,30]. One needs to start from a previously converged solution in the MI and to make small steps in μ in order to numerically reveal the hysteresis.

As expected, on a triangular lattice, the hole- and electron-doped sides are asymmetrical. For these parameters on the electron-doped side, the hysteresis is between a metal and an insulator, as observed on the square lattice with second-neighbor hopping [26,31]. Nevertheless, what looks like a hysteresis between a metal and an insulator in fact evolves continuously into the Sordi transition, as shown in Fig. 2(a) that displays the evolution of the doping-driven transitions as a function of interaction strength U. Even if a first-order metal to insulator transition seems to be more commonly

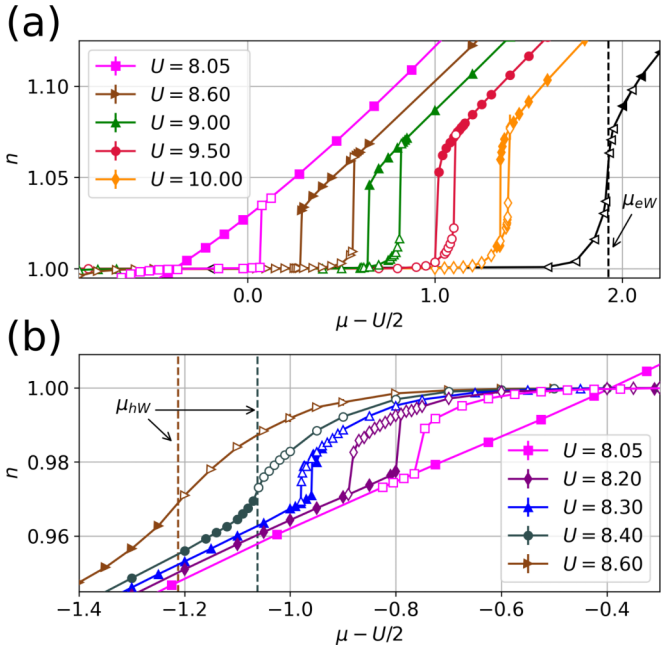

FIG. 2. Evolution of the first-order doping-driven transition with respect to U on the (a) electron- and (b) hole-doped sides at $T = 1/15$. The Widom line μ_{hW} (μ_{eW}) is the value of μ on the hole-doped (electron-doped) side where the compressibility $\partial n/\partial\mu$ is maximal for a given value of U.

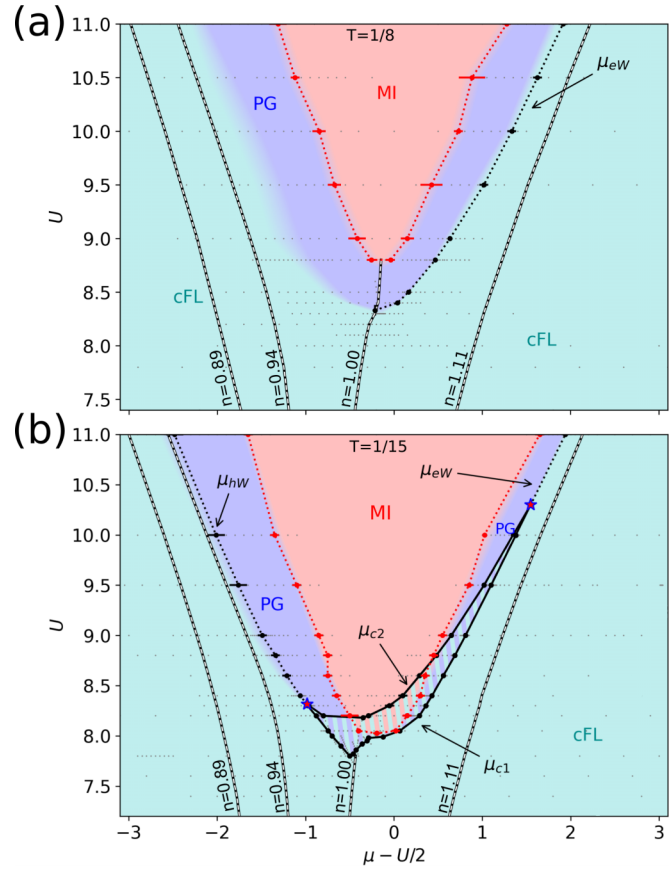

FIG. 3. Phase diagram with U on the vertical axis and $\mu - U/2$ on the horizontal axis for (a) $T = 1/8$ and (b) $T = 1/15$ showing the connections between the MI, Widom lines μ_{eW} and μ_{hW}, and Sordi transitions. Phases are labeled as correlated Fermi liquid (cFL), pseudogap (PG), and Mott insulator (MI). The red stars with blue contours highlight the critical (U, μ) of the Sordi transition where the compressibility tends toward infinity, on both the hole- and electron-doped sides. The color gradients between some of the phases represent the crossover nature of the transitions. The red dotted line represents where the spectral weight at $\omega = 0$ is below a small threshold ($\delta = 0.005$) [38].

witnessed [26,31], increasing U makes it clear that there is a Sordi transition. The Sordi transition was often presented as a transition induced by hole doping [34,53–55], but our results suggest that the transitions on the electron- and hole-doped sides are very similar, even in the case of large electron-hole asymmetry.

Figure 2(b) presents the hole-doped side. We see that the Sordi transition disappears upon increasing U to $U = 8.35 \pm 0.05$ and that it then becomes a Widom line $\mu_{hW}(U)$ [34], which is a line of maxima of thermodynamic quantities [85,86]. In this case, the Widom line is defined as a maximum of the compressibility $\partial n/\partial\mu$ that slowly vanishes as U increases. On the other hand, for U down to $U = 8.05$, once in the metallic state it cannot go back to the insulator. This is the expected behavior when U is in the interval $U_{c1} < U < U_{c2}$, the spinodals of the interaction-driven Mott transition at half-filling. Note that the Sordi transition on the electron-doped side exists at that temperature for a much wider range of interaction ($8.8 \lesssim U \lesssim 10.3$) than on the hole-doped side.

Connection to Mott physics. To better grasp the connection between the Sordi transition, the PG, and Mott physics, we present their interplay on the phase diagrams presented in Fig. 3. It displays the three phases, MI, PG, and cFL, encountered in Fig. 2 for a wide range of μ and U for two different temperatures: $T = 1/8$ in (a) and $T = 1/15$ in (b). Notably, the doping range of the PG decreases with temperature, and the Mott energy gap becomes smaller as the temperature increases. At $T = 1/8$, the phase diagram is rather simple. We find that the Mott gap increases with U, and that a rapid crossover separates the electron-doped PG and the cFL. The physics becomes more interesting when the temperature decreases. At $T = 1/15$, we find that the cFL can coexist with either the PG or the MI, as highlighted by the hatched region. Although we cannot reach infinitesimally small temperatures with continuous-time quantum Monte Carlo, we expect that the Sordi transition likely remains down to $T = 0$ if long-range order does not appear [55]. The portions of this region corresponding to Sordi transitions are those where the hysteresis occurs between the cFL and the PG phases at constant U. The limit between the PG and the cFL are intimately related to the first-order doping-driven transition or to the Widom line.

While the limit between the PG and the cFL is clear when there is a first-order transition, it is no longer the case at large U or high temperature. Indeed, in these cases, the first-order transition evolves into a Widom line or leaves no visible trace in the compressibility $\partial n/\partial\mu$. It makes it particularly hard to define only one objective criterion for the boundary between the PG and the cFL [38]. Another important remark is that the

spinodals μ_{c1} and μ_{c2} of the Sordi transition are connected at half-filling to U_{c1} and U_{c2} discussed in Ref. [23], showing the direct relationship between the Sordi transition and the Mott transition. Finally, we observe around $\mu = 3.4$ and $U = 7.8$ that a PG can be found with a U slightly lower than U_c for the MI. This peninsula in the PG phase has an analog in the 1D Hubbard model [87].

Discussion. Our results provide evidence for Sordi transitions in the triangular Hubbard model using DCA, hence showing that this phenomenon is not an artifact of two-orbital DMFT nor of CDMFT on 2×2 clusters. We stress that our implementation of the CT-AUX impurity solver and DCA algorithm are independent of any previous studies on this subject. Furthermore, many other studies found that the Hubbard model on a triangular lattice does not have long-range magnetic correlations at half-filling in the temperature and interaction regime we study ($\sim$8.2) [61–71]. This suggests that our study is not biased by large correlation lengths, that the Sordi transition is not a magnetic transition, and that it could be measured experimentally.

The Sordi transition separates two different metals: one highly correlated and the other less correlated. The former is interpreted as a PG state, although the formal proof of a **k**-dependent loss of spectral weight remains to be seen and is kept for future works, as it will require additional extensive calculations. Triangular lattices are highly frustrated, thus the existence of the strong-coupling PG in the triangular Hubbard model is strong evidence that long-range magnetic correlations are not a necessary ingredient for the onset of a PG, consistent with other studies [29,33,35,36,88].

As suggested by Fig. 2, the hysteresis associated to the Sordi transition appears to be indissociable from the Mott transition, as follows from the phase diagram, Fig. 3(b), where it clearly emerges from the Mott insulator. This was seen on the square lattice as well [28,29]. At temperatures where DCA calculations can be performed, this hysteresis is found in the low interaction limit of the doped MI [28,29,34,40], but it should persist to larger interactions in lower temperature phase diagrams [28,29]. The transition also disappears when the temperature increases. Furthermore, we find that at $T = 1/15$, the critical μ_{c1} and μ_{c2} of the interaction-driven Mott transition are connected to U_{c1} and U_{c2} of the interaction-driven Mott transition. The PG is constrained within the boundary delimited by μ_{c1}. This is further evidence that the PG is an unavoidable consequence of Mott physics in systems where singlet formation can occur because of strong interactions.

The scenario of a first-order doping-driven transition separating a strongly correlated metal from a weakly correlated one is similar to results for the two-orbital Hubbard model in Ref. [55] where the authors observed the Sordi transition between a strongly correlated Hund metal and a weakly correlated metal. Their conclusion suggests the hypothesis that the two critical points denoted by stars in Fig. 3 are finite temperature critical points that might extend to quantum critical points at zero temperature.

Such fundamental connections between different phenomena have important consequences for our understanding of the Hubbard model and thus of the cuprates, modeled on a square lattice with frustrated hoppings. Having a PG that is unrelated to long-range AFM correlations but that still starts at a critical endpoint suggests that the sudden drop of T^* in cuprates near the critical doping, usually noted p^*, is a signature of Mott physics [40,42,47,48]. Although the physics of the PG on the hole-doped side in our results is relevant for the PG found in hole-doped cuprates [29], our PG on the electron-doped side is not related to the PG of the electron-doped cuprates, since those arise from long wavelength spin fluctuations [33,35,89–92]. In addition, our work is relevant for doped layered organic superconductors [72,73], for field-effect doped organic superconductors [74], for doped 1T-TaS_2 [93] or for analog simulators [94–97]. Our predictions motivate experiments at low temperatures in these systems.

Conclusion. We report the Sordi transition between a strongly correlated pseudogap phase and a correlated Fermi liquid on the triangular lattice Hubbard model at finite temperature. This transition is not an artifact of two-orbital DMFT, nor of 2×2 CDMFT as confirmed by our alternate 6-site DCA approach. We expect that other computational methods will be able to identify this transition on the triangular lattice, contrary to the unfrustrated square lattice where large system size calculations do not even find a Mott transition due to antiferromagnetism [59]. On the triangular lattice, magnetic correlations arising from superexchange are short ranged at finite temperature, so the mechanism for the pseudogap is not related to long-wavelength magnetic fluctuations. Finally, our U-μ phase diagrams show that both this pseudogap and the Sordi transition are phenomena intimately associated to doping a Mott insulator, and as such they should be observable in any dopable system where the Mott transition can be observed at finite temperature. Future work should focus on additional experimental predictions, in particular for layered organic materials.

We thank C. Bourbonnais, J. Fournier, C. Gauvin-Ndiaye, A. Georges, A. Pustogow, P. Rosenberg, T. Schäfer, D. Sénéchal, G. Sordi, and C. Walsh for fruitful discussions. We also thank M. Rousseau for his technical support. The computational resources for this work were provided by Compute Canada and Calcul Québec. We acknowledge support by the Natural Sciences and Engineering Council of Canada through RGPIN-2019-05312 and by the Canada First Research Excellence Fund. The Flatiron Institute is a division of the Simons Foundation. P.-O.D. thanks the "Fonds de recherche du Québec - Nature et technologie (FRQNT)" for a scholarship.

[1] J. Hubbard, Electron correlations in narrow energy bands, Proc. R. Soc. London A **276**, 238 (1963).

[2] J. Hubbard, Electron correlations in narrow energy bands. II. The degenerate band case, Proc. R. Soc. London A **277**, 237 (1964).

[3] J. Hubbard, Electron correlations in narrow energy bands III. An improved solution, Proc. R. Soc. London A **281**, 401 (1964).

[4] M. C. Gutzwiller, Effect of correlation on the ferromagnetism of transition metals, Phys. Rev. Lett. **10**, 159 (1963).

[5] J. Kanamori, Electron correlation and ferromagnetism of transition metals, Prog. Theor. Phys. **30**, 275 (1963).

[6] D. B. McWhan, A. Menth, J. P. Remeika, W. F. Brinkman, and T. M. Rice, Metal-insulator transitions in pure and doped V_2O_3, Phys. Rev. B **7**, 1920 (1973).

[7] X. Granados, J. Fontcuberta, X. Obradors, L. Mañosa, and J. B. Torrance, Metallic state and the metal-insulator transition of $NdNiO_3$, Phys. Rev. B **48**, 11666 (1993).

[8] S. Lefebvre, P. Wzietek, S. Brown, C. Bourbonnais, D. Jérome, C. Mézière, M. Fourmigué, and P. Batail, Mott transition, antiferromagnetism, and unconventional superconductivity in layered organic superconductors, Phys. Rev. Lett. **85**, 5420 (2000).

[9] M. Dumm, D. Faltermeier, N. Drichko, M. Dressel, C. Mézière, and P. Batail, Bandwidth-controlled Mott transition in $\kappa-(BEDT-TTF)_2Cu[N(CN)_2]Br_xCl_{1-x}$: Optical studies of correlated carriers, Phys. Rev. B **79**, 195106 (2009).

[10] K. Kanoda and R. Kato, Mott physics in organic conductors with triangular lattices, Annu. Rev. Condens. Matter Phys. **2**, 167 (2011).

[11] A. Pustogow, M. Bories, A. Löhle, R. Rösslhuber, E. Zhukova, B. Gorshunov, S. Tomić, J. A. Schlueter, R. Hübner, T. Hiramatsu, Y. Yoshida, G. Saito, R. Kato, T.-H. Lee, V. Dobrosavljević, S. Fratini, and M. Dressel, Quantum spin liquids unveil the genuine Mott state, Nat. Mater. **17**, 773 (2018).

[12] E. Gorelov, M. Karolak, T. O. Wehling, F. Lechermann, A. I. Lichtenstein, and E. Pavarini, Nature of the Mott transition in Ca_2RuO_4, Phys. Rev. Lett. **104**, 226401 (2010).

[13] C. S. Alexander, G. Cao, V. Dobrosavljevic, S. McCall, J. E. Crow, E. Lochner, and R. P. Guertin, Destruction of the Mott insulating ground state of Ca_2RuO_4 by a structural transition, Phys. Rev. B **60**, R8422 (1999).

[14] A. Georges and G. Kotliar, Hubbard model in infinite dimensions, Phys. Rev. B **45**, 6479 (1992).

[15] M. Jarrell, Hubbard model in infinite dimensions: A quantum Monte Carlo study, Phys. Rev. Lett. **69**, 168 (1992).

[16] A. Georges, G. Kotliar, W. Krauth, and M. J. Rozenberg, Dynamical mean-field theory of strongly correlated fermion systems and the limit of infinite dimensions, Rev. Mod. Phys. **68**, 13 (1996).

[17] A. M. S. Tremblay, B. Kyung, and D. Sénéchal, Pseudogap and high-temperature superconductivity from weak to strong coupling. Towards a quantitative theory, Low Temp. Phys. **32**, 424 (2006).

[18] J. Vučičević, H. Terletska, D. Tanasković, and V. Dobrosavljević, Finite-temperature crossover and the quantum Widom line near the Mott transition, Phys. Rev. B **88**, 075143 (2013).

[19] H. Park, K. Haule, and G. Kotliar, Cluster dynamical mean field theory of the Mott transition, Phys. Rev. Lett. **101**, 186403 (2008).

[20] M. Balzer, B. Kyung, D. Sénéchal, A.-M. S. Tremblay, and M. Potthoff, First-order Mott transition at zero temperature in two dimensions: Variational plaquette study, Europhys. Lett. **85**, 17002 (2009).

[21] C. Walsh, P. Sémon, D. Poulin, G. Sordi, and A.-M. S. Tremblay, Thermodynamic and information-theoretic description of the Mott transition in the two-dimensional Hubbard model, Phys. Rev. B **99**, 075122 (2019).

[22] H. T. Dang, X. Y. Xu, K.-S. Chen, Z. Y. Meng, and S. Wessel, Mott transition in the triangular lattice Hubbard model: A dynamical cluster approximation study, Phys. Rev. B **91**, 155101 (2015).

[23] P.-O. Downey, O. Gingras, J. Fournier, C.-D. Hébert, M. Charlebois, and A.-M. S. Tremblay, Mott transition, Widom line, and pseudogap in the half-filled triangular lattice Hubbard model, Phys. Rev. B **107**, 125159 (2023).

[24] H. Lee, G. Li, and H. Monien, Hubbard model on the triangular lattice using dynamical cluster approximation and dual fermion methods, Phys. Rev. B **78**, 205117 (2008).

[25] G. Kotliar, S. Murthy, and M. J. Rozenberg, Compressibility divergence and the finite temperature Mott transition, Phys. Rev. Lett. **89**, 046401 (2002).

[26] A. Macridin, M. Jarrell, T. Maier, P. R. C. Kent, and E. D'Azevedo, Pseudogap and antiferromagnetic correlations in the Hubbard model, Phys. Rev. Lett. **97**, 036401 (2006).

[27] E. Gull, O. Parcollet, P. Werner, and A. J. Millis, Momentum-sector-selective metal-insulator transition in the eight-site dynamical mean-field approximation to the Hubbard model in two dimensions, Phys. Rev. B **80**, 245102 (2009).

[28] G. Sordi, K. Haule, and A. M. S. Tremblay, Finite doping signatures of the Mott transition in the two-dimensional Hubbard model, Phys. Rev. Lett. **104**, 226402 (2010).

[29] G. Sordi, K. Haule, and A.-M. S. Tremblay, Mott physics and first-order transition between two metals in the normal-state phase diagram of the two-dimensional Hubbard model, Phys. Rev. B **84**, 075161 (2011).

[30] E. Gull, M. Ferrero, O. Parcollet, A. Georges, and A. J. Millis, Momentum-space anisotropy and pseudogaps: A comparative cluster dynamical mean-field analysis of the doping-driven metal-insulator transition in the two-dimensional Hubbard model, Phys. Rev. B **82**, 155101 (2010).

[31] E. Khatami, K. Mikelsons, D. Galanakis, A. Macridin, J. Moreno, R. T. Scalettar, and M. Jarrell, Quantum criticality due to incipient phase separation in the two-dimensional Hubbard model, Phys. Rev. B **81**, 201101 (2010).

[32] By thermodynamically stable, we mean a phase whose free energy is a global minimum, contrary to metastable phases whose free energy are local minima, thus allowing phase coexistence.

[33] V. Hankevych, B. Kyung, A.-M. Daré, D. Sénéchal, and A.-M. S. Tremblay, Strong- and weak-coupling mechanisms for pseudogap in electron-doped cuprates, J. Phys. Chem. Solids **67**, 189 (2006).

[34] G. Sordi, P. Sémon, K. Haule, and A.-M. S. Tremblay, Pseudogap temperature as a Widom line in doped Mott insulators, Sci. Rep. **2**, 547 (2012).

[35] D. Sénéchal and A.-M. S. Tremblay, Hot spots and pseudogaps for hole- and electron-doped high-temperature superconductors, Phys. Rev. Lett. **92**, 126401 (2004).

[36] B. Kyung, S. S. Kancharla, D. Sénéchal, A.-M. S. Tremblay, M. Civelli, and G. Kotliar, Pseudogap induced by short-range spin correlations in a doped Mott insulator, Phys. Rev. B **73**, 165114 (2006).

[37] Y. M. Vilk and A.-M. S. Tremblay, Non-perturbative many-body approach to the Hubbard model and single-particle pseudogap, J. Phys. I France **7**, 1309 (1997).

[38] See Supplemental Material at http://link.aps.org/supplemental/10.1103/PhysRevB.110.L121109 for more details on densities

of states features that characterize crossovers and the distinctive nature of the pseudogap, which includes Ref. [98].

[39] X. Deng, J. Mravlje, R. Žitko, M. Ferrero, G. Kotliar, and A. Georges, How bad metals turn good: Spectroscopic signatures of resilient quasiparticles, Phys. Rev. Lett. **110**, 086401 (2013).

[40] G. Sordi, P. Sémon, K. Haule, and A.-M. S. Tremblay, *c*-axis resistivity, pseudogap, superconductivity, and Widom line in doped Mott insulators, Phys. Rev. B **87**, 041101 (2013).

[41] G. Sordi, P. Sémon, K. Haule, and A.-M. S. Tremblay, Strong coupling superconductivity, pseudogap, and Mott transition, Phys. Rev. Lett. **108**, 216401 (2012).

[42] A. Reymbaut, S. Bergeron, R. Garioud, M. Thénault, M. Charlebois, P. Sémon, and A.-M. S. Tremblay, Pseudogap, Van Hove singularity, maximum in entropy, and specific heat for hole-doped Mott insulators, Phys. Rev. Res. **1**, 023015 (2019).

[43] C. Walsh, M. Charlebois, P. Sémon, G. Sordi, and A.-M. S. Tremblay, Prediction of anomalies in the velocity of sound for the pseudogap of hole-doped cuprates, Phys. Rev. B **106**, 235134 (2022).

[44] G. Sordi, C. Walsh, P. Sémon, and A.-M. S. Tremblay, Specific heat maximum as a signature of Mott physics in the two-dimensional Hubbard model, Phys. Rev. B **100**, 121105 (2019).

[45] J. Fournier, P.-O. Downey, C.-D. Hébert, M. Charlebois, and A.-M. Tremblay, Two T-linear scattering rate regimes in the triangular lattice Hubbard model, arXiv:2312.08306.

[46] C. Walsh, P. Sémon, G. Sordi, and A.-M. S. Tremblay, Critical opalescence across the doping-driven Mott transition in optical lattices of ultracold atoms, Phys. Rev. B **99**, 165151 (2019).

[47] N. Doiron-Leyraud, O. Cyr-Choinière, S. Badoux, A. Ataei, C. Collignon, A. Gourgout, S. Dufour-Beauséjour, F. F. Tafti, F. Laliberté, M.-E. Boulanger, M. Matusiak, D. Graf, M. Kim, J.-S. Zhou, N. Momono, T. Kurosawa, H. Takagi, and L. Taillefer, Pseudogap phase of cuprate superconductors confined by Fermi surface topology, Nat. Commun. **8**, 2044 (2017).

[48] O. Cyr-Choinière, R. Daou, F. Laliberté, C. Collignon, S. Badoux, D. LeBoeuf, J. Chang, B. J. Ramshaw, D. A. Bonn, W. N. Hardy, R. Liang, J.-Q. Yan, J.-G. Cheng, J.-S. Zhou, J. B. Goodenough, S. Pyon, T. Takayama, H. Takagi, N. Doiron-Leyraud, and L. Taillefer, Pseudogap temperature T^* of cuprate superconductors from the Nernst effect, Phys. Rev. B **97**, 064502 (2018).

[49] G. Campi, M. V. Mazziotti, T. Jarlborg, and A. Bianconi, Scale-free distribution of oxygen interstitial wires in optimum-doped $HgBa_2CuO_{4+y}$, Condensed Matter **7**, 56 (2022).

[50] B. Michon, C. Girod, S. Badoux, J. Kačmarčík, Q. Ma, M. Dragomir, H. A. Dabkowska, B. D. Gaulin, J.-S. Zhou, S. Pyon, T. Takayama, H. Takagi, S. Verret, N. Doiron-Leyraud, C. Marcenat, L. Taillefer, and T. Klein, Thermodynamic signatures of quantum criticality in cuprate superconductors, Nature (London) **567**, 218 (2019).

[51] G. Grissonnanche, Y. Fang, A. Legros, S. Verret, F. Laliberté, C. Collignon, J. Zhou, D. Graf, P. A. Goddard, L. Taillefer, and B. J. Ramshaw, Linear-in temperature resistivity from an isotropic Planckian scattering rate, Nature (London) **595**, 667 (2021).

[52] J. P. L. Faye and D. Sénéchal, Pseudogap-to-metal transition in the anisotropic two-dimensional Hubbard model, Phys. Rev. B **96**, 195114 (2017).

[53] H. Bragança, S. Sakai, M. C. O. Aguiar, and M. Civelli, Correlation-driven Lifshitz transition at the emergence of the pseudogap phase in the two-dimensional Hubbard model, Phys. Rev. Lett. **120**, 067002 (2018).

[54] L. Fratino, S. Bag, A. Camjayi, M. Civelli, and M. Rozenberg, Doping-driven resistive collapse of the Mott insulator in a minimal model for VO_2, Phys. Rev. B **105**, 125140 (2022).

[55] M. Chatzieleftheriou, A. Kowalski, M. Berović, A. Amaricci, M. Capone, L. De Leo, G. Sangiovanni, and L. de' Medici, Mott quantum critical points at finite doping, Phys. Rev. Lett. **130**, 066401 (2023).

[56] G. Kotliar, S. Y. Savrasov, K. Haule, V. S. Oudovenko, O. Parcollet, and C. A. Marianetti, Electronic structure calculations with dynamical mean-field theory, Rev. Mod. Phys. **78**, 865 (2006).

[57] L. Fratino, P. Sémon, G. Sordi, and A.-M. Tremblay, An organizing principle for two-dimensional strongly correlated superconductivity, Sci. Rep. **6**, 22715 (2016).

[58] L. Fratino, P. Sémon, G. Sordi, and A.-M. S. Tremblay, Pseudogap and superconductivity in two-dimensional doped charge-transfer insulators, Phys. Rev. B **93**, 245147 (2016).

[59] T. Schäfer, F. Geles, D. Rost, G. Rohringer, E. Arrigoni, K. Held, N. Blümer, M. Aichhorn, and A. Toschi, Fate of the false Mott-Hubbard transition in two dimensions, Phys. Rev. B **91**, 125109 (2015).

[60] D. J. Schultz, A. Khoury, F. Desrochers, O. Tavakol, E. Z. Zhang, and Y. B. Kim, Electric field control of a quantum spin liquid in weak Mott insulators, Phys. Rev. B **109**, 214423 (2024).

[61] A. Wietek, R. Rossi, F. Šimkovic, M. Klett, P. Hansmann, M. Ferrero, E. M. Stoudenmire, T. Schäfer, and A. Georges, Mott insulating states with competing orders in the triangular lattice Hubbard model, Phys. Rev. X **11**, 041013 (2021).

[62] H. Morita, S. Watanabe, and M. Imada, Nonmagnetic insulating states near the Mott transitions on lattices with geometrical frustration and implications for κ-$(ET)_2Cu_2(CN)_3$, J. Phys. Soc. Jpn. **71**, 2109 (2002).

[63] B. Kyung and A.-M. S. Tremblay, Mott transition, antiferromagnetism, and d-wave superconductivity in two-dimensional organic conductors, Phys. Rev. Lett. **97**, 046402 (2006).

[64] P. Sahebsara and D. Sénéchal, Hubbard model on the triangular lattice: Spiral order and spin liquid, Phys. Rev. Lett. **100**, 136402 (2008).

[65] M. Laubach, R. Thomale, C. Platt, W. Hanke, and G. Li, Phase diagram of the Hubbard model on the anisotropic triangular lattice, Phys. Rev. B **91**, 245125 (2015).

[66] K. Misumi, T. Kaneko, and Y. Ohta, Mott transition and magnetism of the triangular-lattice Hubbard model with next-nearest-neighbor hopping, Phys. Rev. B **95**, 075124 (2017).

[67] L. F. Tocchio, F. Becca, A. Parola, and S. Sorella, Role of backflow correlations for the nonmagnetic phase of the t–t' Hubbard model, Phys. Rev. B **78**, 041101 (2008).

[68] T. Yoshioka, A. Koga, and N. Kawakami, Quantum phase transitions in the Hubbard model on a triangular lattice, Phys. Rev. Lett. **103**, 036401 (2009).

[69] H.-Y. Yang, A. M. Läuchli, F. Mila, and K. P. Schmidt, Effective spin model for the spin-liquid phase of the Hubbard model on the triangular lattice, Phys. Rev. Lett. **105**, 267204 (2010).

[70] A. Szasz, J. Motruk, M. P. Zaletel, and J. E. Moore, Chiral spin liquid phase of the triangular lattice Hubbard model: A density

matrix renormalization group study, Phys. Rev. X **10**, 021042 (2020).

[71] B.-B. Chen, Z. Chen, S.-S. Gong, D. N. Sheng, W. Li, and A. Weichselbaum, Quantum spin liquid with emergent chiral order in the triangular-lattice Hubbard model, Phys. Rev. B **106**, 094420 (2022).

[72] H. Oike, Y. Suzuki, H. Taniguchi, Y. Seki, K. Miyagawa, and K. Kanoda, Anomalous metallic behaviour in the doped spin liquid candidate κ-$(ET)_4Hg_{2.89}Br_8$, Nat. Commun. **8**, 756 (2017).

[73] R. Yoshimoto, A. Naito, S. Yamashita, and Y. Nakazawa, Antiferromagnetic fluctuations and proton Schottky heat capacity in doped organic conductor κ-$(BEDT\text{-}TTF)_4Hg_{2.78}Cl_8$, Phys. B: Condens. Matter **427**, 1 (2013).

[74] H. M. Yamamoto, M. Nakano, M. Suda, Y. Iwasa, M. Kawasaki, and R. Kato, A strained organic field-effect transistor with a gate-tunable superconducting channel, Nat. Commun. **4**, 2379 (2013).

[75] D. P. Arovas, E. Berg, S. Kivelson, and S. Raghu, The Hubbard model, Annu. Rev. Condens. Matter Phys. **13**, 239 (2022).

[76] M. Qin, T. Schäfer, S. Andergassen, P. Corboz, and E. Gull, The Hubbard model: A computational perspective, Annu. Rev. Condens. Matter Phys. **13**, 275 (2022).

[77] J. LeBlanc *et al.* (Simons Collaboration), Solutions of the two-dimensional Hubbard model: Benchmarks and results from a wide range of numerical algorithms, Phys. Rev. X **5**, 041041 (2015).

[78] T. Schäfer, N. Wentzell, F. Šimkovic, Y.-Y. He, C. Hille, M. Klett, C. J. Eckhardt, B. Arzhang, V. Harkov, F.-M. Le Régent, A. Kirsch, Y. Wang, A. J. Kim, E. Kozik, E. A. Stepanov, A. Kauch, S. Andergassen, P. Hansmann, D. Rohe, Y. M. Vilk *et al.*, Tracking the footprints of spin fluctuations: A multi-method, multimessenger study of the two-dimensional Hubbard model, Phys. Rev. X **11**, 011058 (2021).

[79] This is explained in Appendix A of Ref. [23] based on the anisotropic triangular lattice.

[80] M. H. Hettler, M. Mukherjee, M. Jarrell, and H. R. Krishnamurthy, Dynamical cluster approximation: Nonlocal dynamics of correlated electron systems, Phys. Rev. B **61**, 12739 (2000).

[81] T. A. Maier, M. Jarrell, T. Pruschke, and M. Hettler, Quantum cluster theories, Rev. Mod. Phys. **77**, 1027 (2005).

[82] Edited by E. Pavarini, E. Koch, and P. Coleman, in *Many-Body Physics: From Kondo to Hubbard*, Schriften des Forschungszentrums Jülich. Reihe modeling and simulation, Vol. 5, Autumn School on Correlated Electrons, Jülich (Germany), 21 Sep 2015-25 Sep 2015 (Forschungszentrum Jülich GmbH Zentralbibliothek, Verlag, Jülich, 2015).

[83] E. Gull, P. Werner, O. Parcollet, and M. Troyer, Continuous-time auxiliary-field Monte Carlo for quantum impurity models, Europhys. Lett. **82**, 57003 (2008).

[84] E. Gull, A. J. Millis, A. I. Lichtenstein, A. N. Rubtsov, M. Troyer, and P. Werner, Continuous-time Monte Carlo methods for quantum impurity models, Rev. Mod. Phys. **83**, 349 (2011).

[85] L. Xu, P. Kumar, S. V. Buldyrev, S.-H. Chen, P. H. Poole, F. Sciortino, and H. E. Stanley, Relation between the widom line and the dynamic crossover in systems with a liquid-liquid phase transition, Proc. Natl. Acad. Sci. USA **102**, 16558 (2005).

[86] G. G. Simeoni, T. Bryk, F. A. Gorelli, M. Krisch, G. Ruocco, M. Santoro, and T. Scopigno, The widom line as the crossover between liquid-like and gas-like behaviour in supercritical fluids, Nat. Phys. **6**, 503 (2010).

[87] T. Giamarchi, Mott transition in one dimension, Phys. B: Condens. Matter **230-232**, 975 (1997).

[88] F. Simkovic, R. Rossi, A. Georges, and M. Ferrero, Origin and fate of the pseudogap in the doped Hubbard model, arXiv:2209.09237.

[89] C. Gauvin-Ndiaye, M. Setrakian, and A.-M. S. Tremblay, Resilient Fermi liquid and strength of correlations near an antiferromagnetic quantum critical point, Phys. Rev. Lett. **128**, 087001 (2022).

[90] C. Weber, K. Haule, and G. Kotliar, Strength of correlations in electron- and hole-doped cuprates, Nat. Phys. **6**, 574 (2010).

[91] M. Horio, K. P. Kramer, Q. Wang, A. Zaidan, K. von Arx, D. Sutter, C. E. Matt, Y. Sassa, N. C. Plumb, M. Shi, A. Hanff, S. K. Mahatha, H. Bentmann, F. Reinert, S. Rohlf, F. K. Diekmann, J. Buck, M. Kalläne, K. Rossnagel, E. Rienks *et al.*, Oxide Fermi liquid universality revealed by electron spectroscopy, Phys. Rev. B **102**, 245153 (2020).

[92] E. M. Motoyama, G. Yu, I. M. Vishik, O. P. Vajk, P. K. Mang, and M. Greven, Spin correlations in the electron-doped high-transition-temperature superconductor $Nd_{2-x}Ce_xCuO_{4\pm\delta}$, Nature (London) **445**, 186 (2007).

[93] K. T. Law and P. A. Lee, $1T-TaS_2$ as a quantum spin liquid, Proc. Natl. Acad. Sci. USA **114**, 6996 (2017).

[94] F. Ming, S. Johnston, D. Mulugeta, T. S. Smith, P. Vilmercati, G. Lee, T. A. Maier, P. C. Snijders, and H. H. Weitering, Realization of a hole-doped Mott insulator on a triangular silicon lattice, Phys. Rev. Lett. **119**, 266802 (2017).

[95] L. Tarruell and L. Sanchez-Palencia, Quantum simulation of the Hubbard model with ultracold fermions in optical lattices, C. R. Phys., **19**, 365 (2018).

[96] J. Yang, L. Liu, J. Mongkolkiattichai, and P. Schauss, Site-resolved imaging of ultracold fermions in a triangular-lattice quantum gas microscope, PRX Quantum **2**, 020344 (2021).

[97] J. Mongkolkiattichai, L. Liu, D. Garwood, J. Yang, and P. Schauss, Quantum gas microscopy of a geometrically frustrated Hubbard system, Phys. Rev. A **108**, L061301 (2023).

[98] D. Bergeron and A.-M. S. Tremblay, Algorithms for optimized maximum entropy and diagnostic tools for analytic continuation, Phys. Rev. E **94**, 023303 (2016).